JCI The Journal of Clinical Investigation

Notch inhibition overcomes resistance to Tyrosine Kinase Inhibitors in EGFR-driven lung adenocarcinoma

Emilie Bousquet Mur, … , Luis Paz-Ares, Antonio Maraver

J Clin Invest. 2019. https://doi.org/10.1172/JCI126896.

Research In-Press Preview **Oncology**

EGFR mutated lung adenocarcinoma patients treated with gefitinib and osimertinib show a therapeutic benefit limited by the appearance of secondary mutations, such as $EGFR^{T790M}$ and $EGFR^{C797S}$. It is generally assumed that these secondary mutations render EGFR completely unresponsive to the inhibitors, but contrary to this, we uncovered here that gefitinib and osimertinib increased STAT3 phosphorylation (pSTAT3) in $EGFR^{T790M}$ and $EGFR^{C797S}$ tumoral cells. Interestingly, we also found that concomitant Notch inhibition with gefitinib or osimertinib treatment induced a pSTAT3-dependent strong reduction in the levels of the transcriptional repressor HES1. Importantly, we showed that tyrosine kinase inhibitor resistant tumors, with $EGFR^{T790M}$ and $EGFR^{C797S}$ mutations, were highly responsive to the combined treatment of Notch inhibitors with gefitinib and osimertinib respectively. Finally, in patients with EGFR mutations treated with tyrosine kinase inhibitors, HES1 protein levels increased during relapse and correlated with shorter progression-free survival. Therefore, our results offer a proof of concept for an alternative treatment to chemotherapy in lung adenocarcinoma osimertinib treated patients after disease progression.

Notch inhibition overcomes resistance to tyrosine kinase inhibitors in EGFR-driven lung adenocarcinoma

Emilie Bousquet Mur[1], Sara Bernardo[1], Laura Papon[1], Maicol Mancini[1], Eric Fabbrizio[1], Marion Goussard[1], Irene Ferrer[1, 2, 3], Anais Giry[1], Xavier Quantin[1], Jean-Louis Pujol[1, 4], Olivier Calvayrac[5], Herwig P. Moll[6], Yaël Glasson[7], Nelly Pirot[7], Andrei Turtoi[8], Marta Cañamero[9], Kwok-Kin Wong[10], Yosef Yarden[11], Emilio Casanova[6, 12], Jean-Charles Soria[13], Jacques Colinge[14], Christian W. Siebel[15], Julien Mazieres[5, 16], Gilles Favre[5], Luis Paz-Ares[2, 4, 17], Antonio Maraver[1,*]

[1] *Oncogenic pathways in lung cancer, Institut de Recherche en Cancérologie de Montpellier (IRCM), Univ Montpellier, Institut Régional du Cancer de Montpellier (ICM), Montpellier, 34298, Cedex 5, France.*
[2] *Unidad de Investigación Clínica de Cáncer de Pulmón, Instituto de Investigación Hospital 12 de Octubre-CNIO, Madrid, 28029-28041, Spain.*
[3] *CIBERONC, 28029, Madrid, Spain.*
[4] *Montpellier Academic Hospital, Hôpital Arnaud de Villeneuve, 34090, Cedex 5, Montpellier, France.*
[5] *Inserm, Centre de Recherche en Cancérologie de Toulouse, CRCT UMR-1037, Toulouse, France; Institut Claudius Regaud, IUCT-Oncopole, Laboratoire de Biologie Médicale Oncologique, Toulouse, France; University of Toulouse III (Paul Sabatier), Toulouse, France.*
[6] *Department of Physiology, Center of Physiology and Pharmacology and Comprehensive Cancer Center (CCC), Medical University of Vienna, AT-1090 Vienna, Austria*
[7] *Réseau d'Histologie Expérimentale de Montpellier, BioCampus, UMS3426 CNRS-US009 INSERM-UM, Montpellier, France.*
[8] *Tumor microenvironment and resistance to treatment, Institut de Recherche en Cancérologie de Montpellier (IRCM), Univ Montpellier, Institut Régional du Cancer de Montpellier (ICM), Montpellier, 34298, Cedex 5, France.*
[9] *Roche Pharmaceutical Research and Early Development, Translational Medicine, Roche Innovation Center, Munich, Germany.*
[10] *Laura and Isaac Perlmutter Cancer Center, NYU Langone Medical Center, New York, NY 10016, USA.*
[11] *Department of Biological Regulation, Weizmann Institute of Science, Rehovot, 76100, Israel.*
[12] *Ludwig Boltzmann Institute for Cancer Research (LBI-CR), Vienna 1090, Austria.*
[13] *Drug Development Department (DITEP), Gustave Roussy Cancer Campus, Paris-Sud University, Villejuif, 76100, France*
[14] *Cancer bioinformatics and systems biology, Institut de Recherche en Cancérologie de Montpellier (IRCM), Univ Montpellier, Institut Régional du Cancer de Montpellier (ICM), Montpellier, 34298, Cedex 5, France.*
[15] *Department of Discovery Oncology, Genentech, Inc., 1 DNA Way, South San Francisco, CA 94080, USA.*
[16] *Thoracic Oncology Department, Larrey Hospital, University Hospital of Toulouse, France; Inserm, Centre de Recherche en Cancérologie de Toulouse, CRCT UMR-1037, Toulouse, France; University of Toulouse III (Paul Sabatier), Toulouse, France.*
[17] *Medical School, Universidad Complutense, 28040, Madrid, Spain.*

Conflict of interest statement: The authors have declared that no conflict of interest exists.

Correspondence to:

Antonio Maraver, PhD
Oncogenic pathways in lung cancer
Institut de Recherche en Cancérologie de Montpellier
Inserm U1194 - Université Montpellier - ICM
Campus Val d'Aurelle
208 Rue des Apothicaires
F-34298 Montpellier Cedex 5, France
Tel office: +33(0) 467 612 395
Fax: +33(0) 467 613 787
e-mail: antonio.maraver@inserm.fr

ABSTRACT

EGFR mutated lung adenocarcinoma patients treated with gefitinib and osimertinib show a therapeutic benefit limited by the appearance of secondary mutations, such as $EGFR^{T790M}$ and $EGFR^{C797S}$. It is generally assumed that these secondary mutations render EGFR completely unresponsive to the inhibitors, but contrary to this, we uncovered here that gefitinib and osimertinib increased STAT3 phosphorylation (pSTAT3) in $EGFR^{T790M}$ and $EGFR^{C797S}$ tumoral cells. Interestingly, we also found that concomitant Notch inhibition with gefitinib or osimertinib treatment induced a pSTAT3-dependent strong reduction in the levels of the transcriptional repressor HES1. Importantly, we showed that tyrosine kinase inhibitor resistant tumors, with $EGFR^{T790M}$ and $EGFR^{C797S}$ mutations, were highly responsive to the combined treatment of Notch inhibitors with gefitinib and osimertinib respectively. Finally, in patients with EGFR mutations treated with tyrosine kinase inhibitors, HES1 protein levels increased during relapse and correlated with shorter progression-free survival. Therefore, our results offer a proof of concept for an alternative treatment to chemotherapy in lung adenocarcinoma osimertinib treated patients after disease progression.

INTRODUCTION

Lung cancer kills about a million people every year worldwide being the leading cause of death by cancer in the world. Lung cancer consists of two main types: small cell lung carcinoma that accounts for about 20% of lung cancers and the non-small cell lung carcinoma, divided into lung adenocarcinoma, lung squamous carcinoma and large cell carcinoma, that account for around 40%, 30% and 10% of all lung cancer, respectively (1). Genetic alterations in the *EGFR* gene is encountered in about 20% of lung adenocarcinoma patients in Western countries, and up to 50% in some Asian countries such as Korea. The most common ones are deletions in exon 19 and the activating $EGFR^{L858R}$ mutation (2). The life expectancy of this subset of patients has improved dramatically thanks to the development of tyrosine kinase inhibitor (TKI)s (3). Most of the patients treated with first generation TKIs (i.e. gefitinib and erlotinib) initially respond well, however, their tumors rapidly develop resistance. This is explained, in about 60% of cases, by acquisition of the so called 'gatekeeper' mutation $EGFR^{T790M}$ (4). More recently, third-generation TKIs, as osimertinib, targeting $EGFR^{T790M}$ showed very good therapeutic response in patients expressing this mutation (5). Unfortunately, tumors from patients treated with osimertinib also become resistant to this drug; in around 30% of cases this is due to acquisition of new gatekeeper mutations, as $EGFR^{C797S}$ (6, 7). Thus, single drug to treat efficiently EGFR-driven lung adenocarcinoma might have limited value and a strategy based on combinational drug therapy could be more effective at mitigating the effects of gatekeeper mutations.

The resistance conferred by the $EGFR^{T790M}$ gatekeeper mutation is multifactorial including a weaker drug binding trough steric hindrance as well as an increase in the affinity for ATP in EGFR (8). Still, the binding of gefitinib in the presence of the $EGFR^{T790}$ gatekeeper mutation, although negatively affected is not totally inhibited (8).

Even more, X-ray structure indicates that gefitinib binds to EGFR in a similar manner in the presence or absence of $EGFR^{T790M}$ gatekeeper mutation (9). Hence, we hypothesized that although not reaching therapeutic effect, gefitinib could to a certain level impact EGFR downstream signaling pathways and this could be exploited upon combined inhibition of other signaling pathways.

The Notch signaling pathway is highly conserved amongst metazoans and it is important during embryonic development as well as adult tissue homeostasis. In mammals, there are four NOTCH receptors (NOTCH1 to 4), that are activated upon interaction with transmembrane ligands (DELTA and JAGGED). For this activation to occur, an intramembrane protease called γ-secretase, releases the Notch intracytoplasmic domain (NICD) that, upon nuclear translocation and binding to its DNA binding partner RBPJ, modulates the expression of target genes of the canonical Notch pathway, such as HES1 (10). The Notch pathway may thus be inhibited by γ-secretase inhibitors (GSIs) or by antibodies against the ligands or the receptors (11).

By making use of genetically engineered mouse models, we and others have demonstrated that KRAS-driven lung adenocarcinoma are dependent on Notch activity (12-14). Regarding EGFR-driven lung adenocarcinoma, seminal works using cell lines and murine subcutaneous xenografts showed that a combination of Notch inhibitors and EGFR TKIs produces a better response than single treatments in sensitive cells (15-17). However, the mechanism underlying this positive effect is not fully understood, and even more, the role of the Notch pathway in lung adenocarcinoma that relapsed due to acquisition of gatekeeper mutations in *EGFR* remains largely unknown.

In here, several pathways, including the KRAS signaling pathway, were downregulated in transcriptomic analysis performed upon treatment with gefitinib in EGFR-driven lung adenocarcinoma of human cells harboring the $EGFR^{T790M}$ gatekeeper

mutation. Hence, based on our previous work (14), we combined TKIs with Notch inhibition in the presence of EGFR gatekeeper mutations and importantly, re-sensitizes *in vivo* human and murine lung adenocarcinoma resistant to gefitinib via pSTAT3 binding onto the *HES1* promoter, thus repressing HES1 expression. Similarly, Notch inhibition re-sensitizes *in vivo* human lung adenocarcinoma cells harboring $EGFR^{C797S}$ mutation to osimertinib, that most probably will become soon the first line of treatment in EGFR-driven lung adenocarcinoma patients. Altogether, our data show that Notch inhibition could be a potent strategy to treat TKI-resistant EGFR-driven lung adenocarcinoma patients.

RESULTS

Gefitinib treatment in human lung adenocarcinoma cells with the gatekeeper mutation *EGFR^{T790M}* induces changes in several cancer-associated genetic signatures

To identify molecular changes upon gefitinib treatment in lung cancer cells harboring the *EGFR^{T790M}* mutation that confers resistance to first-generation TKIs, we used the already described human EGFR-driven lung adenocarcinoma PC9GR cell line (*EGFR^{T790M}*) resistant to gefitinib (18). Gene set enrichment analysis using the «Molecular Signatures Database Hallmark Gene Set Collection» (19, 20) of data obtained by RNA-seq of PC9GR cells treated with vehicle or gefitinib showed that among the fifty signatures, only one was upregulated (HALLMARK_KRAS_SIGNALING_DN) (Supplemental Table 1). Accordingly, among the eight downregulated gene sets in gefitinib-treated cells, we found "HALLMARK_KRAS_SIGNALING_UP" (Figure 1A and Supplemental Table 1). This suggests that in PC9GR cells, gefitinib decreases the activity of the KRAS signaling pathway, a well-known EGFR downstream pathway (21).

We previously reported that the Notch pathway plays a major role in KRAS-driven lung adenocarcinoma, and that its inhibition fully stops tumor growth in this setting (14). Therefore, we hypothesized that gefitinib effects in PC9GR cells harboring the *EGFR^{T790M}* gatekeeper mutation could be enhanced by Notch inhibition.

Inhibition of Notch signaling hampers tumor growth in *EGFR$^{T790M/L858R}$* mice

Before directly testing this hypothesis, we studied the Notch pathway activation in EGFR-driven lung tumors *in vivo*, by crossing *EGFR$^{T790M/L858R}$* (22) and lung-specific *CCSP-rtTA* transgenic mice (23) to obtain mice in which *EGFR$^{T790M/L858R}$* expression in lungs can be induced by treatment with doxycycline (*EGFR$^{T790M/L858R}$* mice, hereafter). After 8

weeks of doxycycline treatment, mice developed bronchial and peripheral *EGFR*$^{T790M/L858R}$-driven tumors that are resistant to first-generation EGFR TKIs, such as gefitinib (22). Western blot analysis showed that N1ICD, the processed and active form of NOTCH1, and HES1, a Notch target gene, were strongly expressed in *EGFR*$^{T790M/L858R}$-driven tumors compared with normal lung tissue from control mice (either littermates with the same genotype but not treated with doxycycline, or CCSP-rtTA transgenic mice treated with doxycycline) (Figure 1B). This finding is similar to what observed in the *Kras*^{G12V} mouse model (14), and suggests that the Notch pathway may play a similar role in both tumor types.

As the NOTCH1 and NOTCH3 receptors promote *Kras*^{G12V}-driven lung adenocarcinoma, whereas NOTCH2 has a tumor suppressive role (12, 13, 24), we analyzed their expression in *EGFR*$^{T790M/L858R}$-driven lung adenocarcinoma. The transmembrane forms of NOTCH1 and NOTCH3 (i.e., before γ-secretase cleavage) were strongly expressed in tumor samples compared with controls (Figure 1B), whereas NOTCH2 expression was comparable in both groups (Figure 1B). Although the level of the transmembrane forms of NOTCH receptors does not reflect Notch activity, and NOTCH3 can be a direct target of NOTCH1 in some circumstances, this finding suggests that both NOTCH1 and NOTCH3 are mediators of the Notch pathway in EGFR-driven tumors *in vivo*.

To test whether Notch pathway activity is necessary for the growth of EGFR-driven tumors, we treated *EGFR*$^{T790M/L858R}$ mice with doxycycline for 8 weeks to induce tumor formation, and then randomly assigned them to three groups: i) control group, treated with vehicle and IgG antibody control; ii) GSI group, treated with dibenzazepine (DBZ), a potent and selective GSI; and iii) anti-NRR1/NRR3 group, treated with blocking antibodies against NOTCH1 and NOTCH3, according to previously described treatment

regimens (25-27). After five weeks of treatment, tumors represented more than 40% of the lung area in the control group, but only 20% and 10% in the DBZ and anti-NRR1/NRR3 groups, respectively (Figure 1C). This indicates that the Notch pathway is required for $EGFR^{T790M/L858R}$-driven tumor growth. Body weight was comparable in the three groups (Supplemental Figure 1A), suggesting the absence of the intestinal toxicity reported by other studies using regimens that led to stronger Notch inhibition (28).

As expected, analysis of protein expression by immunohistochemistry (IHC) of tumors from anti-NRR1/NRR3- or DBZ- treated mice showed fewer HES1-positive cells than in the vehicle-treated control group, implying that these treatments effectively inhibited the Notch pathway (Figure 1D). Moreover, the percentage of Ki67-positive cells was lower in tumors from the anti-NRR1/NRR3 and DBZ groups than the control group, indicating that Notch activity promotes cell proliferation in $EGFR^{T790M/L858R}$-driven tumors (Figure 1D). As the MAPK and AKT pathways are crucial downstream players of the EGFR signaling pathway (21), we also analyzed the expression of pERK and pAKT in the same samples. The percentage of pERK-positive cells was similarly reduced by treatment with the anti-NRR1 and -NRR3 antibodies and with DBZ compared control (Figure 1D), consistent with previous observations (13, 14). Conversely, the percentage of pAKT-positive cells was comparable in all groups (Supplemental Figure 1B).

Notch inhibition overcomes resistance to gefitinib in $EGFR^{T790M/L858R}$–driven lung adenocarcinoma

To study whether pharmacological inhibition of the Notch pathway *in vivo* had any impact on the resistance to gefitinib conferred by the gatekeeper mutation $EGFR^{T790M}$, we randomized $EGFR^{T790M/L858R}$ mice (after 8 weeks of doxycycline treatment) in four

treatment groups: i) vehicle (control), ii) gefitinib, iii) DBZ, and iv) gefitinib + DBZ. For simplicity we decided to inhibit the Notch pathway hereafter only with a GSI.

As before, body weight was comparable in the different groups after the five weeks of treatment, suggesting that these drugs were well tolerated alone or in combination (Supplemental Figure 2A). In agreement with the previous findings (Figure 1C), tumor tissue occupied 42% of the lung in the control group, whereas it was decreased to 23% in the DBZ group (Figure 2A). As expected, gefitinib alone did not have any anti-tumor effect in $EGFR^{T790M/L858R}$ mice (52% of lung was tumor tissue). Conversely, the DBZ and gefitinib combination led to a very significant reduction of the tumor area compared with DBZ alone (tumor tissue covered only 10% of the total lung area) (Figure 2A).

Histopathological analysis of lung adenocarcinoma samples (i.e., non-benign tumors, Supplemental Figure 2B) showed that the single treatments had no effect on the lung adenocarcinoma number compared with control (i.e., vehicle-treated mice) (Figure 2B). Importantly, animals treated with the combination of gefitinib and Notch inhibition had significantly fewer lung adenocarcinomas than vehicle-treated ones (a mean of 10 lung adenocarcinoma per mouse *vs* 31 in the control, Figure 2B).

IHC analysis showed that the percentage of HES1-, Ki67-, pERK- and pAKT-positive cells was comparable in tumors from the gefitinib group and from controls (Figure 2C). By contrast, the percentage of HES1-, Ki67- and pERK-positive cells was reduced in tumors from DBZ-treated mice (Figure 2C), as before (Figure 1D), although in this case the difference was not significant for pERK. The percentage of HES1-, Ki67- and pERK-positive cells tended to be lower in mice treated with the gefitinib and DBZ combination compared with DBZ-treated mice, particularly for pERK. Finally, the percentage of pAKT-positive cells was comparable in the DBZ, gefitinib and control

groups, but interestingly, it was significantly reduced in the gefitinib + DBZ group compared with control mice (Figure 2C).

Altogether, these data demonstrate that inhibition of Notch signaling by DBZ restores sensitivity to treatment with gefitinib in $EGFR^{T790M/L858R}$-driven lung adenocarcinoma *in vivo*.

Notch inhibition overcomes resistance to gefitinib in lung adenocarcinoma patient-derived xenografts with $EGFR^{T790M/L858R}$ mutations

These results were very encouraging; however, it is considered that the best strategy for testing innovative cancer treatments is the combination of genetic mouse models and patient-derived xenograft (PDX) preclinical models (29). Therefore, we developed a lung adenocarcinoma PDX that harbors the $EGFR^{T790M/L858R}$ mutations, like our transgenic mouse model. One week after subcutaneous grafting of the PDX, nude mice were randomized in four groups as before: i) vehicle alone (control), ii) gefitinib, iii) DBZ, and iv) gefitinib + DBZ. Tumor growth was monitored for 30 days (i.e., the treatment duration). As expected, the $EGFR^{T790M}$ mutation conferred resistance to gefitinib. On the other hand, DBZ inhibited tumor growth, and strikingly, the DBZ and gefitinib combination almost totally blocked tumor growth (Figure 3A).

As before, IHC analysis of tumors showed that DBZ (alone or in combination with gefitinib) efficiently decreased the percentage of HES1-positive cells compared with control (Figure 3B). Tumor cell proliferation (Ki67-positive cells) was reduced by DBZ alone, and this effect was increased by addition of gefitinib. Similarly, the percentage of pERK-positive cells was decreased by treatment with DBZ alone and even more by the DBZ and gefitinib combination compared with control. This indicated that the DBZ and gefitinib combination was more effective in reducing MAPK signaling than Notch

inhibition alone. Finally, the percentage of pAKT-positive cells also was efficiently and similarly reduced by DBZ and by the DBZ and gefitinib combination.

Altogether, our results provide strong preclinical evidence for the likely therapeutic benefit of Notch inhibition and gefitinib combination in patients with TKI-resistant EGFR-driven lung adenocarcinoma harboring the gatekeeper mutation $EGFR^{T790M}$.

Combining EGFR TKIs and Notch inhibitors synergistically decreases HES1 expression

Our previous analysis showed that the DBZ and gefitinib combination is more efficient than each single treatment in reducing MAPK and AKT pathways. Previous reports, including work from our laboratory, identified HES1 as an important positive MAPK regulator in KRAS-driven lung adenocarcinoma (13, 30). Even more, HES1 has a similar effect on AKT signaling in T-cell acute lymphoblastic leukemia (T-ALL) (31). Therefore, we hypothesized that HES1 could be an important mediator of pERK and pAKT upon treatment with the DBZ and gefitinib combination. As the percentage of HES1-positive cells was similar in tumors from mice treated with DBZ alone and the DBZ and gefitinib combination in both preclinical models (Figure 2C and Figure 3B), we analyzed HES1 signal intensity in the same samples. Importantly, HES1 signal intensity was significantly lower in tumors from mice treated with the DBZ and gefitinib combination than from mice treated with DBZ alone in the PDX model, and followed a similar trend in $EGFR^{T790M/L858R}$ mice (Figure 4, A and B).

To further validate our data, we analyzed HES1 expression by western blotting in PC9GR cells (previously used for the RNA-seq analysis, Figure 1A and Supplemental Table 1) after incubation with the different drugs alone or in combination. In accordance

to our *in vivo* observation, HES1 expression was strongly reduced in cells exposed to the DBZ and gefitinib combination (Figure 4C).

Then, to explore HES1 role in PC9GR cells, we depleted HES1 using a pool of siRNAs targeting *HES1* mRNA (*siHES1*) (Supplemental Figure 3). Of note, proliferation of *siHES1*-treated cells was impaired compared with control cells transfected with the non-targeted siRNA (*siNT*), and this effect was potentiated in the presence of gefitinib (Figure 4D).

To test whether gefitinib effect was EGFR-mediated, we used the Chinese hamster ovary (CHO) cell line that is a natural null for EGFR, and was previously used for EGFR gain of function analyses (32). Interestingly, HES1 expression was not affected by co-treatment with DBZ and gefitinib in CHO cells transfected with empty vector, but was reduced in CHO cells that express $EGFR^{T790M/L858R}$ protein (Figure 4E). We concluded that EGFR is needed for HES1 expression reduction by the DBZ and gefitinib combination.

Taken together, our data indicate that the DBZ and gefitinib combination synergistically reduces the expression of HES1, a major driver in lung adenocarcinoma.

pSTAT3 directly binds to the *HES1* promoter and inhibits its expression

Previous studies have shown a benefit of combining EGFR TKIs and Notch inhibitors in TKI-sensitive cells, but the underlying mechanism was not fully described (15-17). On the basis of the EGFR-dependent HES1 decrease in $EGFR^{T790M/L858R}$-expressing CHO cells upon incubation with the DBZ and gefitinib combination, we hypothesized that a common mechanism could be involved in the response to TKI treatment in TKI-sensitive and -resistant lung adenocarcinoma cells. An increase in the phosphorylation of STAT3 protein (pSTAT3), dependent on both JAK and FGFR activities, is reported in sensitive

lung adenocarcinoma cells upon treatment with first-generation (erlotinib) and second-generation (afatinib) TKIs (33-35), hence, we investigated whether this occurred also in TKI-resistant cells.

Indeed, analysis of STAT3 phosphorylation status in PC9GR cells showed an increase in pSTAT3 levels upon gefitinib treatment (Figure 5A). This effect was partially inhibited by co-treatment with PD173074 or ruxolitinib, pan-inhibitors of FGFR and JAK pathways respectively. Even more, the combination of both inhibitors reduced pSTAT3 to levels lower than in control non-treated cells (Supplemental Figure 4). Moreover, we found that in the human *HES1* and mouse *Hes1* gene promoters, consensus binding sites for pSTAT3 (i.e., TTNNNNNAA) (36) are close to RBPJ sites (i.e., where the Notch transcription complex binds) (Supplemental Figure 5, A and B). To test whether pSTAT3 binds directly to the human *HES1* promoter in PC9GR cells, we performed chromatin immunoprecipitation (ChIP) experiments using antibodies against pSTAT3 and against NOTCH1, which is known to bind to the *HES1* promoter (positive control). NOTCH1 bound to the *HES1* promoter, and this interaction was reduced by incubation with DBZ (Figure 5B). Importantly, pSTAT3 bound to the *HES1* promoter only when cells were co-incubated with gefitinib and DBZ (Figure 5B). To determine whether pSTAT3 binding was critical for HES1 downregulation (Figure 4C), we incubated PC9GR cells with the various drug combinations after *siSTAT3* treatment that efficiently reduced both pSTAT3 and STAT3 expression (Figure 5C). Co-incubation with gefitinib and DBZ strongly reduced HES1 protein level in control *siNT*-treated cells (Figure 5C), but strikingly, the same co-treatment kept HES1 levels in *siSTAT3*-treated cells (Figure 5C).

Altogether, these findings support that pSTAT3 decreases HES1 protein level by acting as a transcriptional repressor at the *HES1* promoter.

Notch inhibition overcomes resistance to osimertinib in human lung adenocarcinoma cells harboring the *EGFR* ^{C797S} mutation

As various TKIs increase pSTAT3 levels in lung adenocarcinoma cells (33-35), we asked whether the pSTAT3-dependent mechanism observed for gefitinib applied also to osimertinib. To this aim, we used the PC9GROR cell line (previously generated from PC9GR cells) that is resistant to osimertinib and harbor the gatekeeper mutation *EGFR*^{C797S} (18).

First, western blot analysis of PC9GROR cells incubated with DBZ and/or osimertinib showed that pSTAT3 levels increased upon osimertinib treatment. Accordingly, the combination of DBZ and osimertinib reduced HES1 protein levels (Figure 6A).

To test whether DBZ re-sensitized *EGFR*^{C797S} mutant human lung adenocarcinoma cells to osimertinib *in vivo*, we grafted PC9GROR cells subcutaneously in mice, and two weeks later, we treated them with DBZ and/or osimertinib for 3 weeks. Body weight remained comparable in the different treatment groups (Supplemental Figure 6A). Osimertinib alone had no significant effect on growth of PC9GROR cell xenografts (Figure 6B), while it strongly inhibited the growth of PC9GR xenografts (Supplemental Figure 6B). Similarly, DBZ showed no effect on growth of PC9GROR cell xenografts, but importantly, tumor growth was strongly inhibited in mice treated with the osimertinib and DBZ combination (Figure 6B).

This finding demonstrates that treatment with DBZ restores sensitivity to osimertinib in human lung adenocarcinoma cells harboring the *EGFR*^{C797S} mutation, confirming and extending our previous observations that DBZ sensitizes TKI-resistant tumors to TKIs.

Nirogacestat overcomes resistance to gefitinib in human lung adenocarcinoma cells harboring the *EGFR*^{T790M} mutation

To strengthen the translational impact of our work, we wanted to confirm the Notch inhibitor sensitizing effect using a GSI under clinical trials. We chose nirogacestat because a recently finished phase 2 trial, showed that it has promising effects in patients with desmoid tumors, is well tolerated, and can be used for long-term treatments (37).

We randomized mice with subcutaneous PC9GR cell xenografts in six treatment groups: i) vehicle, ii) DBZ, iii) nirogacestat, iv) gefitinib, v) DBZ + gefitinib, vi) and nirogacestat + gefitinib. As gefitinib has some effect in PC9GR cells *in vitro* (Figure 4D), we used 10 mg/kg instead of the previously used dose of 20mg/kg. This lower concentration had a mild, non-significant effect on tumor growth compared with vehicle. Like in PC9GROR cells, the GSIs alone (DBZ and nirogacestat) did not have any effect. Conversely, gefitinib in combination with DBZ or nirogacestat strongly inhibited tumor growth (Figure 7A), as observed in mice harboring PDX and *EGFR*$^{T790M/L858R}$-driven tumors treated with the gefitinib and DBZ combination.

Moreover, Kaplan-Meier survival analysis of mice treated or not with nirogacestat and/or gefitinib showed that survival rate was comparable in mice treated with vehicle, nirogacestat or gefitinib alone, although it tended to be higher in the gefitinib group (Figure 7B). By contrast, the nirogacestat with gefitinib combination increased survival compared with all other groups (median survival after treatment started: 24, 26.5, 32, and 39 days for vehicle, nirogacestat, gefitinib, and nirogacestat + gefitinib, respectively). For this analysis, we used only nirogacestat because at the used dose we could administer DBZ only for 5 weeks (26), while nirogacestat is well tolerated in patients for more than 2 years (37). As before, body weight was not significantly different in all groups during the experiment (Supplemental Figure 7).

These results show that the combination of gefitinib and nirogacestat increases the survival of mice xenografted with human lung adenocarcinoma cells that carry the $EGFR^{T790M}$ mutation conferring resistance to EGFR TKIs.

High HES1 protein levels correlate with poor progression-free survival and relapse in patients with EGFR mutated lung adenocarcinoma treated with TKIs

Our findings showed that HES1 has a key role in the resistance of EGFR-driven lung adenocarcinoma to TKI therapy. To strengthen this observation, we analyzed the correlation between progression-free survival (PFS) and nuclear HES1 protein levels in 75 patients with lung adenocarcinoma harboring *EGFR* mutations and treated with TKIs. We found that patients with low nuclear HES1 expression had a median PFS of 14 months, whereas patients with high nuclear HES1 expression had a median PFS of 7 months (hazard ratio 2.77, 95% CI [1.4-5.5], p = 0.006) (Figure 7C). Moreover, analysis of HES1 protein in tumor biopsy samples from patients with lung adenocarcinoma harboring *EGFR* activating mutations and treated with TKIs taken at diagnosis and after disease progression showed that HES1 nuclear levels were increased in samples obtained at relapse in six of the seven patients (p = 0.034) (Figure 7D and Supplemental Figure 8).

These findings extend our previous study (14), and suggest a crucial role for HES1 in the relapse of patients with EGFR-driven lung adenocarcinoma under treatment with TKIs.

DISCUSSION

In this study, we have extended the role of HES1 as a crucial mediator of the oncogenic activity of the Notch pathway in lung adenocarcinoma and uncover its crucial role in resistance to EGFR TKIs.

We first observed that in EGFR-driven lung adenocarcinoma, treatment with γ-secretase inhibitors produce a decrease in HES1 expression concomitant with a decrease in pERK protein levels. This is consistent with the HES1 induced repression of DUSP1 that in turn, would increase pERK levels as previously described in KRAS-driven lung adenocarcinoma (13, 14). Hence, we assume this is the main mechanism also for the antitumor effect of Notch inhibition as single treatment in EGFR-driven tumors.

Next, as a proof of concept of re-sensitizing cells with EGFR gatekeeper mutations to TKIs upon Notch inhibition, we found that murine and human EGFR-driven lung tumors harboring the $EGFR^{T790M}$ gatekeeper mutation are re-sensitized to gefitinib upon combination with the γ-secretase inhibitor DBZ. Concomitantly, we found that pAKT and pERK where also further decreased upon combined treatment of gefitinib and DBZ, compared to DBZ single treatment. It is reported that HES1 represses PTEN with increasing AKT activity in T-ALL (31) and HES1 also increase pERK levels in lung adenocarcinoma (30). Interestingly, we found in both transgenic- and PDX-preclinical mouse models a decreased expression of HES1 levels in the combination of DBZ and gefitinib compared to DBZ single treatment. Using loss of function analysis, we also found that cells are sensitized to gefitinib in the absence of HES1. Why HES1 loss of function could promote this sensitivity beyond pAKT and pERK? For instance, it is reported in T-ALL that HES1 directly repress *BBC3* gene (i.e. PUMA) an inducer of apoptosis (38), so it is tempting to speculate that HES1 could repress also *BBC3* gene or

other important apoptotic inducers in this context, as for instance *BCL2L11* (i.e. BIM), crucial in gefitinib-induced cell death (39-41).

EGFR^{T790M} mutation does not totally inhibit the binding of gefitinib to the EGFR protein (8, 9), and even more, EGFR was needed in further lowering HES1 expression in the co-treatment of gefitinib and DBZ compared to DBZ alone. Since an increase in active STAT3 upon treatment with both first and second generation TKIs is reported (33-35), we hypothesized that this feature could explain the decreased levels of HES1 in our experimental setting. Indeed, gefitinib treatment of our *EGFR*^{T790M} mutant cell model increased pSTAT3 protein levels in an FGFR and JAK activity dependent manner. Also, a direct recruitment of pSTAT3 was detected onto the *HES1* promoter by ChIP only when gefitinib was combined with GSI. And finally, loss of function of STAT3 maintains HES1 protein in the co-treated cells at similar levels to those in cells treated with DBZ alone. Our data show that pSTAT3 needs a concomitant inhibition of NOTCH processing to repress HES1 expression effectively, probably because the NOTCH transcriptional complex binds more efficiently than pSTAT3. A previous report showed that erlotinib treatment increased the Notch pathway after several days in EGFR-driven lung adenocarcinoma sensitive cells (16). We do not see such induction and this discrepancy could be due to the different treatment kinetics and/or the resistant background of PC9GR cells. Our data are in accordance with the work developed by others, both in the function of pSTAT3 as a transcriptional repressor (42), and in its tumor suppressive role in some types of cancer, including prostate (43), glioblastoma (44), and importantly, KRAS-driven lung adenocarcinoma (45). In light of these data, STAT3 inhibitors currently in clinical trials (46) should be used with caution, at least in those tumors where the Notch pathway, and hence HES1, play a pro-tumorigenic role as in lung adenocarcinoma.

Our findings provide a proof of concept for sensitizing lung adenocarcinoma cells with gatekeeper mutations to TKIs by inhibiting γ-secretase. To extend and validate our findings, we performed an additional assay in lung adenocarcinoma cells with the osimertinib-resistant gatekeeper mutation $EGFR^{C797S}$. The relevance of this experiment relies in results from a recent Phase 3 clinical trial showing that the PFS of patients with EGFR mutations when treated with osimertinib as a first-line treatment was significantly longer than those patients treated in first line with gefitinib or erlotinib (47). Hence, most probably the use of osimertinib as first-line treatment in EGFR mutated lung adenocarcinoma patients will start soon. Our data show that osimertinib treatment in lung adenocarcinoma cells harboring the $EGFR^{C797S}$ mutation induced also pSTAT3 and inhibits HES1 expression, when combined with DBZ. More importantly, also induced a strong tumor growth inhibition of the same cells *in viv*o. Hence, we predict a scenario where osimertinib will bind poorly to EGFR due to the lack of covalent binding induced by $EGFR^{C797S}$ gatekeeper mutation but still would be enough to promote similar changes as those we found in $EGFR^{T790M}$ cells treated with gefitinib and they will be also exacerbated in the presence of Notch inhibition. Our results call for the question regarding the effect of the Notch pathway in the drug-tolerant state (48) in lung adenocarcinoma cells under osimertinib treatment and this is currently an important area of study in the laboratory.

Overall, the mechanistic data described above depict a role for HES1 in relapse to EGFR TKI therapy, and accordingly, we show a negative correlation between HES1 expression and PFS as well as an increase in HES1 expression upon disease progression in EGFR-mutated patients being treated with TKIs. Our results are in accordance with a recent publication that shows a negative correlation between *HES1 mRNA* levels and PFS

418 in a cohort of 64 EGFR mutated non-small cell lung carcinoma patients treated with TKIs
419 (49).

420 Our findings might be very relevant for EGFR-driven lung adenocarcinoma that
421 relapse to osimertinib using gatekeeper mutations as $EGFR^{C797S}$, where treatment
422 possibilities are mainly limited to conventional therapies, since immune check-point
423 inhibitors are mostly ineffective in this context. Our findings warrant the development of
424 a Phase 1 clinical trial to prove the efficacy of the GSI–TKI drug combination in patients.
425 Interestingly, a phase I/II trial in 16 patients that combined the TKI erlotinib and the GSI
426 from Roche, RO4929097, showed that this combination was safe and feasible in lung
427 adenocarcinoma patients (50). As the side effects associated with erlotinib are higher than
428 those with osimertinib (47), a combination of osimertinib with GSIs is also likely to be
429 safe in patients. For instance, with nirogacestat that showed long-term efficacy and is well
430 tolerated in patients (37), and even more, we demonstrated in here it sensitizes human
431 lung adenocarcinoma cells harboring gatekeeper mutations against TKIs.

MATERIAL AND METHODS

Mice

Tet-on-EGFR$^{T790M/L858R}$ and CCSP-rtTA mice were described previously (22, 23). For in vivo PC9GR, PC9GROR lung adenocarcinoma cells tumor growth assays, six-week-old, female athymic Nude-Foxn1 mice (Envigo) were injected subcutaneously in the flank with 3.5 x 10^6 PC9GR or PC9GROR cells. Drug treatments were started when tumors were 200 mm^3. In Kaplan-Meier analysis mice were killed when tumors arise to 1200 mm^3.

Animal procedures were performed according to protocols approved by the French national committee of animal care.

Western blotting

Western blotting was performed as previously described (14). The following antibodies were used for the analysis: N1ICD (#4147, Cell Signaling Technology, USA, 1:500 dilution), HES1 (#11988, Cell Signaling Technology, 1:1000 dilution), NOTCH1 (#3608, Cell Signaling Technology, 1:1.000 dilution), NOTCH2 (#5732, Cell Signaling Technology, 1:1000 dilution), NOTCH3 (#5276, Cell Signaling Technology, 1:1.000 dilution), pSTAT3 (#9145, Cell Signaling Technology, 1:1000 dilution), total STAT3 (#610189, BD, USA, 1:1000 dilution), tubulin (#T9026, Sigma, 1:2000 dilution). Secondary antibodies were either horseradish peroxidase-linked anti-rabbit (#7077, Cell Signaling Technology, 1:10000 dilution), or anti-mouse (#7076, Cell Signaling Technology, 1:10000 dilution). Antibody binding was detected by chemiluminescence using the ECL detection system (GE Healthcare) or ECL Plus (for N1ICD) (GE Healthcare).

Treatments in mice

Dibenzazepine (DBZ) (Syncom) and nirogacestat (MedChemExpress) was administered 4 days per week (3.3 and 50 mg/kg/day respectively) by intraperitoneal (IP) injection or gavage respectively. Gefitinib and osimertinib (Cliniscience) was administered by gavage 4 days a week (20 mg/kg/day) and 5 days a week (5 mg/kg/day) respectively. Antibodies against NOTCH1 (NRR1) and NOTCH3 (NRR3) were administered by IP injection: NRR1 at 5 mg/kg/day every 5 days and NRR3 at 15 mg/kg/day every Monday and Thursday (Genentech).

Histopathology and immunohistochemistry

Lung lobes were fixed, embedded in paraffin and stained with hematoxylin and eosin (HE) or used for immunohistochemistry. Tumor area and total lung area were measured using Image J software. For pathological analysis of HE, classical cytological and architectural features (as invasion or high mitotic rate) were examined by our expert pathologist (M.C.). For immunohistochemistry, the following antibodies were used: rabbit monoclonal anti- HES1 (1:1000 dilution, #11988 from Cell Signaling Technology); rat monoclonal anti- Ki67 (1:100 dilution, #TEC-3 from Agilent, USA); rabbit polyclonal anti-phospho-p44/42 Erk1/Erk2 (Thr202/Tyr204 and Thr185/Tyr187, respectively) (1:25 dilution, #9101 from Cell Signaling Technology); and rabbit monoclonal anti-phospho-Akt1 (Ser473) (1:175 dilution, clone EP2109Y from Novus Biologicals, USA). For each tumor, five 10X magnification fields were scored using Image J software. For the intensity, both in murine and clinical samples, a score (0, for the lowest intensity and 5, for the highest) was given.

Cell culture and transfection reagents

PC9GR (resistant to gefitinib), and PC9GROR (resistant to gefitinib and osimertinib) were obtained from the lab of Y.Y. (18). The siRNA control (non-targeting, *siNT*), and against *HES1* (*siHES1*) or *STAT3* (*siSTAT3*) (Dharmacon) were transfected at 20 nM with Dharmafect1 following the manufacturer's instructions.

For western blotting, RNAseq or ChIP, cells were treated with DBZ (250 nM) (or DMSO as vehicle), gefitinib (1 μM), osimertinib (250 nM), PD173074 (2μM) or ruxolitinib (0.25 μM), the last two molecules were obtained from Cliniscience. For the siRNA proliferation assay, cells were treated with gefitinib (15 nM) (or DMSO as vehicle). The cells were fixed at various time points and stained with sulforhodamine B (SRB). Absorbance was measured at 560 nm in a microplate reader (Glomax, Promega).

RNA sequencing

RNA was sequenced by Fasteris (Switzerland) using Next-Generation DNA sequencing (NGS) based on Illumina technology. The RNA-seq data were deposited in the National Center for Biotechnology Information's Gene Expression Omnibus (accession number GSE117846).

Reads were aligned against the Ensembl *Homo sapiens* genome assembly (GRCh38). Read counts were extracted from the STAR output file with HTSeq and only the protein-coding genome features were taken into account in the final count matrix.

Sample count normalization was realized by summing read counts for each sample $(s_i, i = 1, \dots, 12)$, computing a first factor for each sample $f_i = s_i / \text{median}_{j=1,\dots,12}(s_j)$. These factors were normalized such that the product of all the normalized factors g_i is equal to 1: $g_i = \frac{f_i}{\sqrt[1/12]{\prod_{j=1,\dots,12} f_j}}$. Finally, each column (each sample) of the read count matrix was divided by the corresponding g_i. We analyzed for gene set enrichment

analysis (19) using « The Molecular Signatures Database Hallmark Gene Set Collection » (20).

Chromatin immunoprecipitation

The chromatin was prepared as described previously (51). We used the ChIP-Adem-Kit and ChIP DNA Prep Adem-Kit (Ademtech) for chromatin immunoprecipitation (ChIP) and DNA purification, respectively, on an AutoMag robot, according the manufacturer's instructions. The anti-NOTCH1 antibody was purchased from Abcam (#ab27525) and the anti-phospho-STAT3 from Cell Signaling Technology (#9145). The immunoprecipitated DNA was analyzed by PCR using:

Prom*HES1* Fw: GAAGGCAATTTTTCCTTTTTC

Prom*HES1* Rev: AAGTTCCCGCTCAGACTTTAC

Patient-derived xenograft model

Patient-derived xenograft (PDX) was generated in the laboratory of L.P-A. at the Instituto de Biomedicina de Sevilla (IBIS). The tumor had a TNM of T2a N1 M0. A piece of 0.5 mm^3 was implanted into the right flanks of six-week-old, female athymic Nude-Foxn1 mice (Envigo), and after two weeks, the mice were randomized and the treatments started.

Patients and ethical considerations

Tumors were analyzed from patients with EGFR mutations and treated with EGFR TKIs. Seventy-five patients were being treated at Toulouse University Hospital (52), and four had participated in the MOSCATO (NCT01566019) or MATCH-R (NCT02517892) clinical trials at the Institut Gustave Roussy. All patients had signed an informed consent form permitting analyses of tissues. This study was approved by the Committee for the

Protection of Persons of each institution and by the French National Agency for Medicines and Health Products Safety (ANSM).

Statistical analysis

Unless otherwise specified, the data are presented as means ± S.E.M. One way analysis of variance (ANOVA) followed by Tukey's post hoc test was performed to assess the significance of expression levels in IHC, as well as to determine the differences among groups for changes in size of tumors or animal weight. In figures 3A, 4D, 6B and 7A, a repeated measures two-way ANOVA followed by Tukey's post hoc test was performed. In Figures 7B and 7C, we analyzed the results with a Gehan–Breslow–Wilcoxon test. Hazard ratio was calculated using Mantel-Haenszel test. In Figure 7D data was analyzed by paired two-tailed Student's t test. Samples (cells or mice) were allocated to their experimental groups according to their pre-determined type (cell type or mouse treatment). Investigators were blinded to the experimental groups in the analysis of data presented in Figures 1C, 1D, 2A, 2B, 2C, 3B, 4A, 4B, 5D, 7C and 7D. In the rest they were not blinded.

$p \leq 0.1$; * $p \leq 0.05$; ** $p \leq 0.01$; *** $p \leq 0.001$, **** $p \leq 0.0001$.

ACKNOWLEDGMENTS

We thank Daniel Herranz, Laurent Le Cam, Daniel Fisher, Hélène Tourriere and Manuel Serrano for helpful discussion and critical reading of the manuscript. Elisabetta Andermarcher professionally edited the manuscript. We thank Dom Helmlinger for technical help with the RNAseq. We thank Simon Cabello-Aguilar for his help uploading the RNAseq into GEO. We thank the IRCM's animal facility unit members for their outstanding work. We thank the immunohistochemistry technical service of Cell Signaling Technology for their help and the immunohistochemistry platform at CNIO for their work. E.B. was supported by a contract from *Fondation de France*. S.B. was supported by a fellowship from the French Ministry of Education and Research. M.M. is supported by a fellowship from *Fondation ARC*. Work in A.M.'s lab is supported by the *Fondation ARC* (PJA 20131200405), the European Commission (CIG631431), the *Institute de Cancer de Montpellier* (ICM) *Fondation*, and the *Institut National du Cancer* (INCa_9257 and SIRIC Montpellier Cancer Grant INCa_Inserm_DGOS_1255). The funders had no role in study design, data collection and analysis, decision to publish, or preparation of the manuscript. E.B. designed and performed most experiments, analyzed data and wrote the manuscript. S.B. performed the experiments for RNAseq and, together with L.P., performed some experiments. M.M. M.G. and A.G. performed some *in vivo* treatments. E.F. performed ChIP experiments. I.F., and L.P-A developed and performed the PDX experiments. X.Q., J-L. P., O.C., J-C. S., J.M. and G.F. performed experiments on clinical samples. M.C. performed the immunohistochemistry analysis of mouse tumors. H.P.M and E.C. supervised the experiments with STAT3. Y.G. and N.P. performed some IHC experiments. K-K.W. supervised the experiments on $EGFR^{T790M/L858R}$ mice. A.T. and J.C. performed the RNAseq analysis. C.S. supervised the experiments with NRR1 and NRR3 antibodies. A.M. designed and supervised the study,

573 secured funding, analyzed data and wrote the manuscript. All authors discussed the results
574 and commented on the manuscript.

REFERENCES

1. Herbst RS, Heymach JV, and Lippman SM. Lung cancer. *N Engl J Med.* 2008;359(13):1367-80.
2. Rosell R, Bivona TG, and Karachaliou N. Genetics and biomarkers in personalisation of lung cancer treatment. *Lancet.* 2013;382(9893):720-31.
3. Reck M, Heigener DF, Mok T, Soria JC, and Rabe KF. Management of non-small-cell lung cancer: recent developments. *Lancet.* 2013;382(9893):709-19.
4. Tan CS, Gilligan D, and Pacey S. Treatment approaches for EGFR-inhibitor-resistant patients with non-small-cell lung cancer. *Lancet Oncol.* 2015;16(9):e447-59.
5. Janne PA, Yang JC, Kim DW, Planchard D, Ohe Y, Ramalingam SS, et al. AZD9291 in EGFR inhibitor-resistant non-small-cell lung cancer. *N Engl J Med.* 2015;372(18):1689-99.
6. Thress KS, Paweletz CP, Felip E, Cho BC, Stetson D, Dougherty B, et al. Acquired EGFR C797S mutation mediates resistance to AZD9291 in non-small cell lung cancer harboring EGFR T790M. *Nat Med.* 2015;21(6):560-2.
7. Le X, Puri S, Negrao MV, Nilsson M, Robichaux JP, Boyle TA, et al. Landscape of EGFR -dependent and -independent resistance mechanisms to osimertinib and continuation therapy post-progression in EGFR-mutant NSCLC. *Clin Cancer Res.* 2018.
8. Yun CH, Mengwasser KE, Toms AV, Woo MS, Greulich H, Wong KK, et al. The T790M mutation in EGFR kinase causes drug resistance by increasing the affinity for ATP. *Proc Natl Acad Sci U S A.* 2008;105(6):2070-5.
9. Yoshikawa S, Kukimoto-Niino M, Parker L, Handa N, Terada T, Fujimoto T, et al. Structural basis for the altered drug sensitivities of non-small cell lung cancer-associated mutants of human epidermal growth factor receptor. *Oncogene.* 2013;32(1):27-38.
10. Bray SJ. Notch signalling in context. *Nat Rev Mol Cell Biol.* 2016;17(11):722-35.
11. Takebe N, Miele L, Harris PJ, Jeong W, Bando H, Kahn M, et al. Targeting Notch, Hedgehog, and Wnt pathways in cancer stem cells: clinical update. *Nat Rev Clin Oncol.* 2015;12(8):445-64.
12. Licciulli S, Avila JL, Hanlon L, Troutman S, Cesaroni M, Kota S, et al. Notch1 is required for Kras-induced lung adenocarcinoma and controls tumor cell survival via p53. *Cancer Res.* 2013;73(19):5974-84.
13. Baumgart A, Mazur PK, Anton M, Rudelius M, Schwamborn K, Feuchtinger A, et al. Opposing role of Notch1 and Notch2 in a Kras-driven murine non-small cell lung cancer model. *Oncogene.* 2014.
14. Maraver A, Fernandez-Marcos PJ, Herranz D, Canamero M, Munoz-Martin M, Gomez-Lopez G, et al. Therapeutic Effect of gamma-Secretase Inhibition in Kras(G12V)-Driven Non-Small Cell Lung Carcinoma by Derepression of DUSP1 and Inhibition of ERK. *Cancer Cell.* 2012;22(2):222-34.
15. Konishi J, Yi F, Chen X, Vo H, Carbone DP, and Dang TP. Notch3 cooperates with the EGFR pathway to modulate apoptosis through the induction of bim. *Oncogene.* 2010;29(4):589-96.
16. Arasada RR, Amann JM, Rahman MA, Huppert SS, and Carbone DP. EGFR blockade enriches for lung cancer stem-like cells through Notch3-dependent signaling. *Cancer Res.* 2014;74(19):5572-84.

17. Hu S, Fu W, Li T, Yuan Q, Wang F, Lv G, et al. Antagonism of EGFR and Notch limits resistance to EGFR inhibitors and radiation by decreasing tumor-initiating cell frequency. *Sci Transl Med.* 2017;9(380).
18. Mancini M, Gal H, Gaborit N, Mazzeo L, Romaniello D, Salame TM, et al. An oligoclonal antibody durably overcomes resistance of lung cancer to third-generation EGFR inhibitors. *EMBO Mol Med.* 2018;10(2):294-308.
19. Subramanian A, Tamayo P, Mootha VK, Mukherjee S, Ebert BL, Gillette MA, et al. Gene set enrichment analysis: A knowledge-based approach for interpreting genome-wide expression profiles. *Proceedings of the National Academy of Sciences.* 2005;102(43):15545-50.
20. Liberzon A, Birger C, Thorvaldsdottir H, Ghandi M, Mesirov JP, and Tamayo P. The Molecular Signatures Database (MSigDB) hallmark gene set collection. *Cell Syst.* 2015;1(6):417-25.
21. Arteaga CL, and Engelman JA. ERBB receptors: from oncogene discovery to basic science to mechanism-based cancer therapeutics. *Cancer Cell.* 2014;25(3):282-303.
22. Li D, Shimamura T, Ji H, Chen L, Haringsma HJ, McNamara K, et al. Bronchial and peripheral murine lung carcinomas induced by T790M-L858R mutant EGFR respond to HKI-272 and rapamycin combination therapy. *Cancer Cell.* 2007;12(1):81-93.
23. Tichelaar JW, Lu W, and Whitsett JA. Conditional expression of fibroblast growth factor-7 in the developing and mature lung. *J Biol Chem.* 2000;275(16):11858-64.
24. Zheng Y, de la Cruz CC, Sayles LC, Alleyne-Chin C, Vaka D, Knaak TD, et al. A rare population of CD24(+)ITGB4(+)Notch(hi) cells drives tumor propagation in NSCLC and requires Notch3 for self-renewal. *Cancer Cell.* 2013;24(1):59-74.
25. Choy L, Hagenbeek TJ, Solon M, French D, Finkle D, Shelton A, et al. Constitutive NOTCH3 Signaling Promotes the Growth of Basal Breast Cancers. *Cancer Res.* 2017;77(6):1439-52.
26. Rivera-Torres J, Guzman-Martinez G, Villa-Bellosta R, Orbe J, Gonzalez-Gomez C, Serrano M, et al. Targeting gamma-secretases protect against angiotensin II-induced cardiac hypertrophy. *J Hypertens.* 2015;33(4):843-50.
27. Wu Y, Cain-Hom C, Choy L, Hagenbeek TJ, de Leon GP, Chen Y, et al. Therapeutic antibody targeting of individual Notch receptors. *Nature.* 2010;464(7291):1052-7.
28. van Es JH, van Gijn ME, Riccio O, van den Born M, Vooijs M, Begthel H, et al. Notch/gamma-secretase inhibition turns proliferative cells in intestinal crypts and adenomas into goblet cells. *Nature.* 2005;435(7044):959-63.
29. Day CP, Merlino G, and Van Dyke T. Preclinical mouse cancer models: a maze of opportunities and challenges. *Cell.* 2015;163(1):39-53.
30. Maraver A, and Serrano M. Notching up a new therapeutic strategy for Non-Small Cell Lung Carcinoma (NSCLC). *Oncotarget.* 2012.
31. Palomero T, Sulis ML, Cortina M, Real PJ, Barnes K, Ciofani M, et al. Mutational loss of PTEN induces resistance to NOTCH1 inhibition in T-cell leukemia. *Nat Med.* 2007;13(10):1203-10.
32. Lo HW, Hsu SC, Ali-Seyed M, Gunduz M, Xia W, Wei Y, et al. Nuclear interaction of EGFR and STAT3 in the activation of the iNOS/NO pathway. *Cancer Cell.* 2005;7(6):575-89.

33. Kim SM, Kwon OJ, Hong YK, Kim JH, Solca F, Ha SJ, et al. Activation of IL-6R/JAK1/STAT3 signaling induces de novo resistance to irreversible EGFR inhibitors in non-small cell lung cancer with T790M resistance mutation. *Mol Cancer Ther.* 2012;11(10):2254-64.
34. Lee HJ, Zhuang G, Cao Y, Du P, Kim HJ, and Settleman J. Drug resistance via feedback activation of Stat3 in oncogene-addicted cancer cells. *Cancer Cell.* 2014;26(2):207-21.
35. Codony-Servat C, Codony-Servat J, Karachaliou N, Molina MA, Chaib I, Ramirez JL, et al. Activation of signal transducer and activator of transcription 3 (STAT3) signaling in EGFR mutant non-small-cell lung cancer (NSCLC). *Oncotarget.* 2017;8(29):47305-16.
36. Darnell JE, Jr. STATs and gene regulation. *Science.* 1997;277(5332):1630-5.
37. Kummar S, O'Sullivan Coyne G, Do KT, Turkbey B, Meltzer PS, Polley E, et al. Clinical Activity of the gamma-Secretase Inhibitor PF-03084014 in Adults With Desmoid Tumors (Aggressive Fibromatosis). *J Clin Oncol.* 2017;35(14):1561-9.
38. Schnell SA, Ambesi-Impiombato A, Sanchez-Martin M, Belver L, Xu L, Qin Y, et al. Therapeutic targeting of HES1 transcriptional programs in T-ALL. *Blood.* 2015;125(18):2806-14.
39. Gong Y, Somwar R, Politi K, Balak M, Chmielecki J, Jiang X, et al. Induction of BIM Is Essential for Apoptosis Triggered by EGFR Kinase Inhibitors in Mutant EGFR-Dependent Lung Adenocarcinomas. *PLOS Medicine.* 2007;4(10):e294.
40. Costa DB, Halmos B, Kumar A, Schumer ST, Huberman MS, Boggon TJ, et al. BIM Mediates EGFR Tyrosine Kinase Inhibitor-Induced Apoptosis in Lung Cancers with Oncogenic EGFR Mutations. *PLOS Medicine.* 2007;4(10):e315.
41. Cragg MS, Kuroda J, Puthalakath H, Huang DCS, and Strasser A. Gefitinib-Induced Killing of NSCLC Cell Lines Expressing Mutant EGFR Requires BIM and Can Be Enhanced by BH3 Mimetics. *PLOS Medicine.* 2007;4(10):e316.
42. Zhang H, Hu H, Greeley N, Jin J, Matthews AJ, Ohashi E, et al. STAT3 restrains RANK- and TLR4-mediated signalling by suppressing expression of the E2 ubiquitin-conjugating enzyme Ubc13. *Nat Commun.* 2014;5:5798.
43. Pencik J, Schlederer M, Gruber W, Unger C, Walker SM, Chalaris A, et al. STAT3 regulated ARF expression suppresses prostate cancer metastasis. *Nat Commun.* 2015;6:7736.
44. Peixoto P, Blomme A, Costanza B, Ronca R, Rezzola S, Palacios AP, et al. HDAC7 inhibition resets STAT3 tumorigenic activity in human glioblastoma independently of EGFR and PTEN: new opportunities for selected targeted therapies. *Oncogene.* 2016;35(34):4481-94.
45. Grabner B, Schramek D, Mueller KM, Moll HP, Svinka J, Hoffmann T, et al. Disruption of STAT3 signalling promotes KRAS-induced lung tumorigenesis. *Nat Commun.* 2015;6:6285.
46. Johnson DE, O'Keefe RA, and Grandis JR. Targeting the IL-6/JAK/STAT3 signalling axis in cancer. *Nat Rev Clin Oncol.* 2018;15(4):234-48.
47. Soria JC, Ohe Y, Vansteenkiste J, Reungwetwattana T, Chewaskulyong B, Lee KH, et al. Osimertinib in Untreated EGFR-Mutated Advanced Non-Small-Cell Lung Cancer. *N Engl J Med.* 2018;378(2):113-25.
48. Sharma SV, Lee DY, Li B, Quinlan MP, Takahashi F, Maheswaran S, et al. A chromatin-mediated reversible drug-tolerant state in cancer cell subpopulations. *Cell.* 2010;141(1):69-80.

49. Codony-Servat J, Codony-Servat C, Cardona AF, Gimenez-Capitan A, Drozdowskyj A, Berenguer J, et al. Cancer Stem Cell Biomarkers in EGFR-Mutation-Positive Non-Small-Cell Lung Cancer. *Clin Lung Cancer.* 2019;20(3):167-77.
50. Gold KA, Byers LA, Fan YH, Fujimoto J, Tse WH, Lee JJ, et al. A phase I/II trial combining erlotinib with gamma secretase inhibitor RO4929097 in advanced non-small cell lung cancer (NSCLC). *Journal of Clinical Oncology.* 2013;31(15_suppl):8104-.
51. Fabbrizio E, El Messaoudi S, Polanowska J, Paul C, Cook JR, Lee JH, et al. Negative regulation of transcription by the type II arginine methyltransferase PRMT5. *EMBO Rep.* 2002;3(7):641-5.
52. Calvayrac O, Mazieres J, Figarol S, Marty-Detraves C, Raymond-Letron I, Bousquet E, et al. The RAS-related GTPase RHOB confers resistance to EGFR-tyrosine kinase inhibitors in non-small-cell lung cancer via an AKT-dependent mechanism. *EMBO Mol Med.* 2017;9(2):238-50.

FIGURES

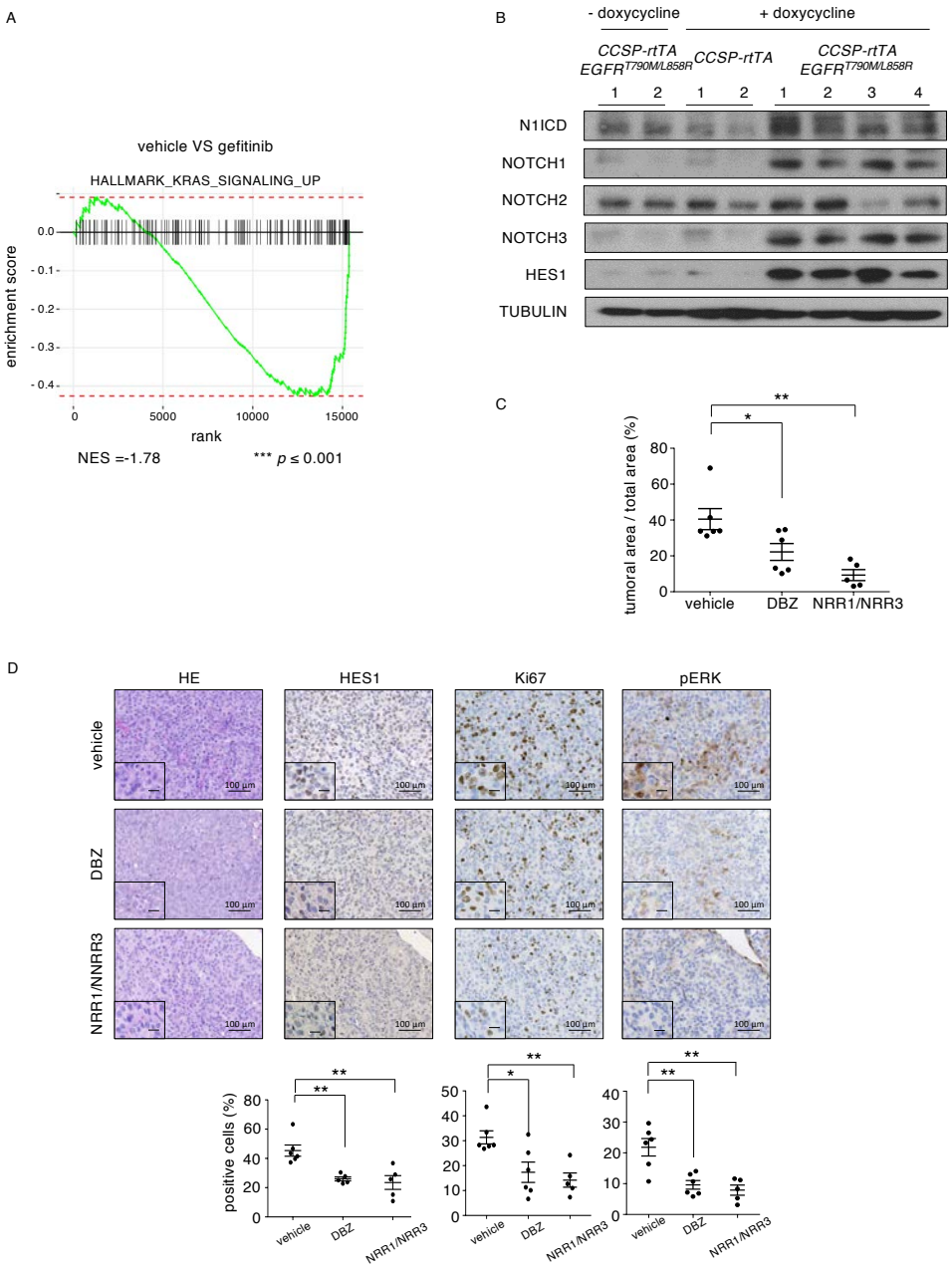

Figure. 1. Inhibition of Notch signaling hampers tumor growth in *EGFR*$^{T790M/L858R}$ mice.

(A) PC9GR cells were starved for 18h and then treated for 6h with vehicle (DMSO) or gefitinib (1 μM). RNA was extracted from cells and subjected to RNAseq. KRAS associated Gene Set was downregulated in PC9GR cells treated with gefitinib (n = 3 per genotype; FDR < 0.001). **(B)** Immunoblotting of the indicated proteins in lungs from control mice and in $EGFR^{T790M/L858R}$-driven tumors (n = 4). The controls were littermates of $EGFR^{T790M/L858R}$ mice that were not induced with doxycycline (n = 2) or CCSP-rtTA mice treated with doxycycline (n = 2). **(C)** Tumor area as a percentage of total lung area of mice treated with methocel and IgG (vehicle; n = 6), with γ-secretase inhibitor (DBZ; n = 6), or with anti-NOTCH1 and anti-NOTCH3 antibodies (NRR1/NRR3; n = 5) was determined by staining tissue sections with H&E. **(D)** H&E (HE) and immunohistochemical staining of lung tumors from the same mice as in **C**. The dot plots show the percentage of positive cells in the corresponding immunohostochemically stained sections. They correspond to the analysis of 5 fields (10X) per tumor. Scale bar at insets = 25μm. Values correspond to the average ± SEM. Statistical significance in C and D was determined by a one-way ANOVA test followed by Tukey's post hoc test: * $p \leq 0.05$, ** $p \leq 0.01$.

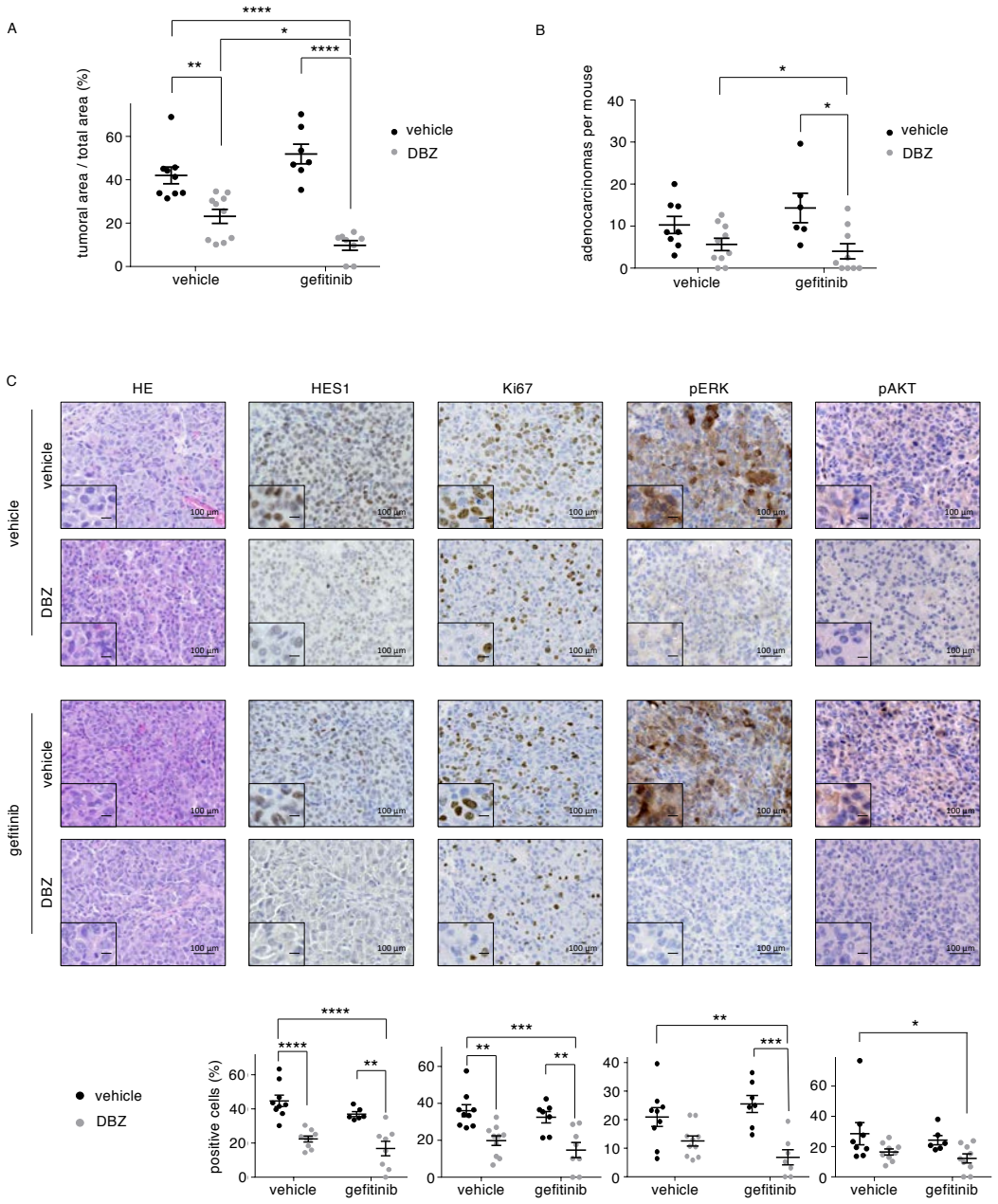

Figure. 2. Notch inhibition sensitizes mouse *EGFR* $^{T790M/L858R}$-driven tumors to gefitinib.

(A) Tumor area as a percentage of the total lung area in sections of lung tissue from mice treated with methocel (vehicle; n = 9), with γ-secretase inhibitor (DBZ; n = 10), with gefitinib (n = 7), or with a combination of DBZ and gefitinib (n = 8) as determined by staining tissue sections with H&E. **(B)** The numbers of lung adenocarcinomas in the same mice as in **A**. **(C)** H&E (HE) and immunohistochemical staining of tumors from the same mice as in **A**. The dot plots show the percentage of positive cells in the corresponding immunohostochemically stained sections. They correspond to the analysis of 5 fields (10X) per tumor. Scale bar at insets = 25μm. Values correspond to the average ± SEM. Statistical significance in **A**, **B** and **C** was determined by one-way ANOVA test followed by Tukey's post hoc test: * $p \leq 0.05$, ** $p \leq 0.01$, *** $p \leq 0.001$ and **** $p \leq 0.0001$. In panel 2A, the comparison between gefitinib and DBZ single treatments was also significant (****). In panel 2C, the comparison between gefitinib alone and DBZ alone for HES1 and p-ERK stainings were also significant (* and ** respectively).

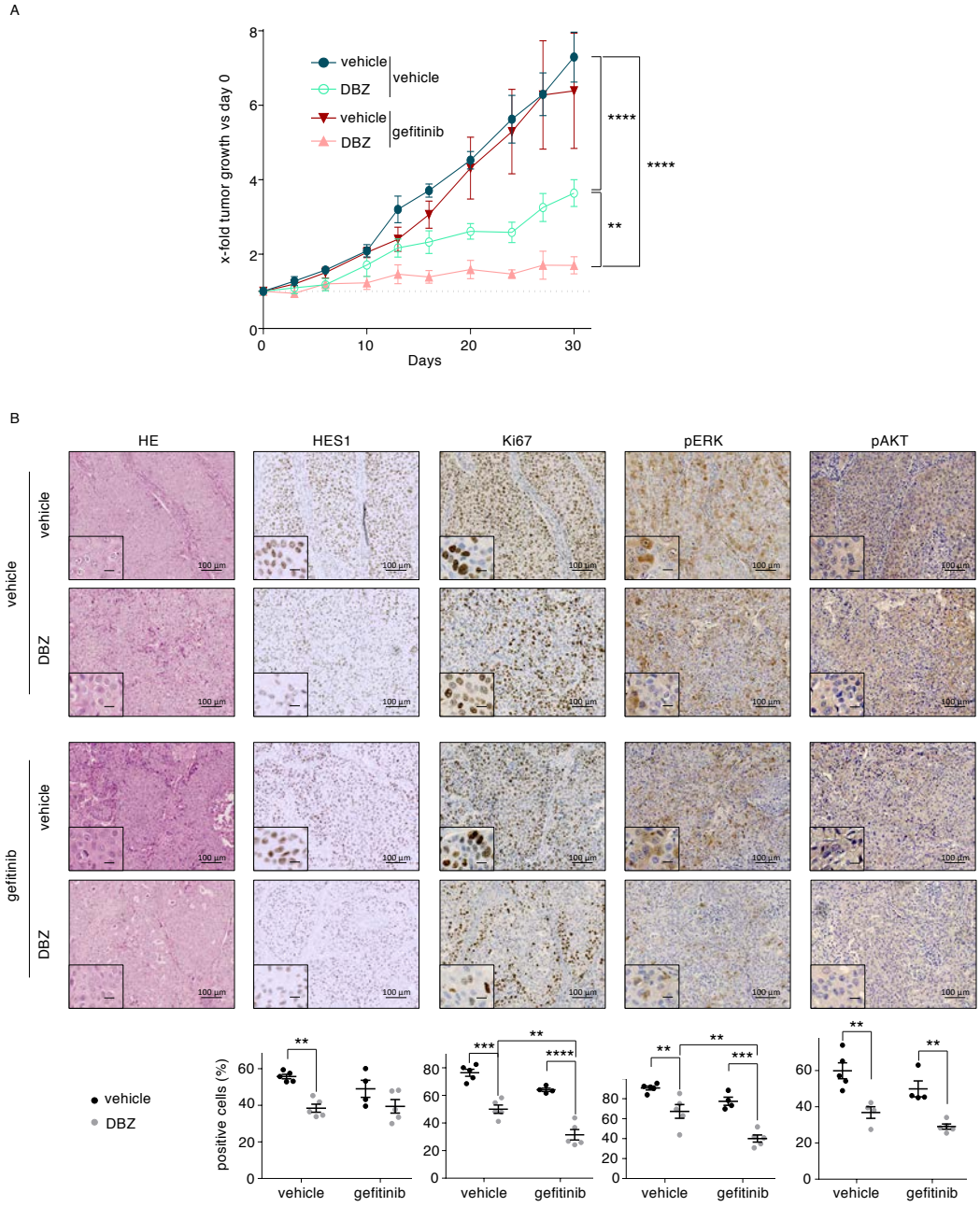

Figure. 3. Notch inhibition sensitizes human *EGFR* $^{T790M/L858R}$-driven lung adenocarcinoma to gefitinib.

(A) Growth of PDX lung adenocarcinoma *EGFR*$^{T790M/L858R}$ implanted in the right flanks of nude mice treated with vehicle (methocel, n = 5), DBZ (n = 5), gefitinib (n = 4) or a combination of DBZ and gefitinib (n = 5). The x-axis shows the fold-increase in tumor size versus day 0. **(B)** H&E (HE) and immunohistochemical staining of tumors from the same mice as in **A**. The dot plots show the percentage of positive cells in the corresponding immunohostochemically stained sections. For each treatment to the analysis of 5 fields (10X) per mouse. Scale bar at insets = 25μm. Values correspond to the average ± SEM. Statistical significance was determined by two-way ANOVA test in **A** and one-way ANOVA in **B** followed by Tukey's post hoc test in both cases: * $p \leq 0.05$, ** $p \leq 0.01$, *** $p \leq 0.001$ and **** $p \leq 0.0001$. In panel 3A, the comparisons between gefitinib single treatment and DBZ or the combination was also significant (respectively *** and ****). In panel 3B, the comparison between vehicle and DBZ was also significant for all stains (** for HES1 and **** for Ki67, p-ERK and p-AKT). Finally, the comparison between gefitinib and DBZ for Ki67 staining was also significant (*).

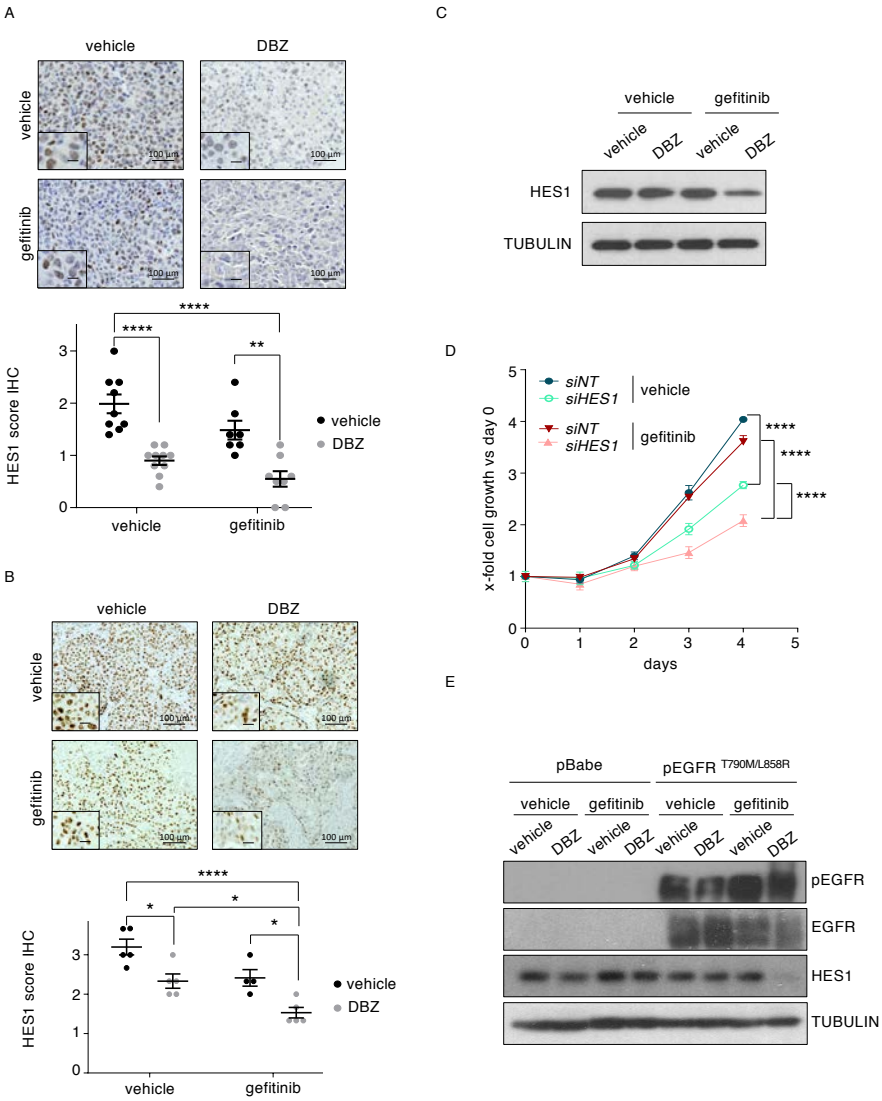

Figure. 4. Combining EGFR TKIs and Notch inhibitors synergistically decreases HES1 expression.

(A) Immunohistochemical staining of HES1 in tumors from *EGFR* $^{T790M/L858R}$ mice treated with methocel (vehicle; n = 9), DBZ (n = 10), gefitinib (n = 7), or with a combination of DBZ and gefitinib (n = 8). **(B)** Immunohistochemical staining of HES1 in tumors from *EGFR*$^{T790M/L858R}$ PDX implanted in nude mice and treated with vehicle (methocel, n = 5), DBZ (n = 5), gefitinib (n = 4) or the combination (n = 5). In **A** and **B**, the dot plots show quantification of the intensity of the staining from the analysis of 5 fields (10 X) per mouse. Scale bar at insets = 25μm. **(C)** Immunoblotting of the indicated proteins in PC9GR cells treated with vehicle (DMSO), DBZ (250 nM) or gefitinib (1 μM). This is a representative image of three different experiments. **(D)** Proliferation of PC9GR cells transfected with a non-targeting siRNA (*siNT*) or targeting *HES1* (*siHES1*) and treated with vehicle (DMSO) or gefitinib (15 nM) for 72 h. The data shown are means ± SEM (n = 3 in all groups). **(E)** Immunoblotting of the indicated proteins in CHO cells transfected with pBabe empty vector or p*EGFR*$^{T790M/L858R}$ and treated with vehicle (DMSO) or DBZ (250 nM) and/or gefitinib (1 μM). This is a representative image of two different experiments.

Values correspond to the average ± SEM. Statistical significance was analyzed by one-way ANOVA test in **A** and **B**, and two-way ANOVA in D followed by Tukey's post hoc test in all cases: * $p \leq 0.05$, ** $p \leq 0.01$, *** $p \leq 0.001$ and **** $p \leq 0.0001$. In the panel 4A, the comparison between gefitinib alone and DBZ alone is also significant (*). In the panel 4B, the comparison between vehicle and gefitinib is also significant (*). And in the panel 4D, the comparison between vehicle with gefitinib alone or vehicle with siHes1/gefitinib or gefitinib with siHes1 are also significant (respectively **, **** and ****).

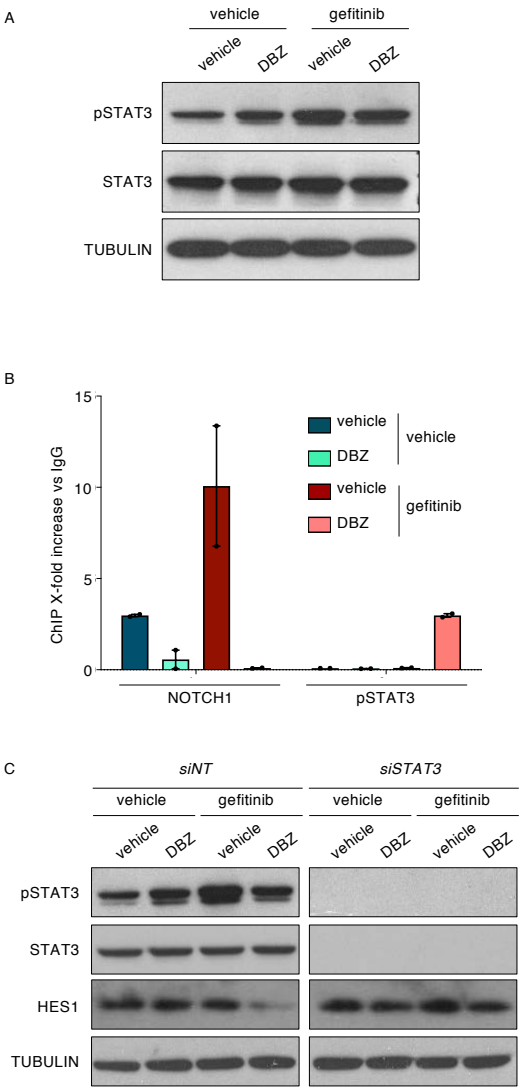

Figure. 5. pSTAT3 directly binds to the *HES1* promoter and inhibits its expression.

(A) Immunoblotting of the indicated proteins in PC9GR cells treated with vehicle (DMSO) or DBZ (250 nM) and/or gefitinib (1 μM). This is a representative image of three different experiments. **(B)** ChIP analysis of the binding of NOTCH1 and pSTAT3 to the *HES1* promoter in PC9GR cells treated as in **A** (n = 2 per treatment). **(C)** Immunoblotting of the indicated proteins in PC9GR cells transfected with a non-targeting siRNA (*siNT*) or targeting *STAT3* (*siSTAT3*) and treated with vehicle (DMSO) or DBZ (250 nM) and/or gefitinib (1 μM). This is a representative image of two different experiments.

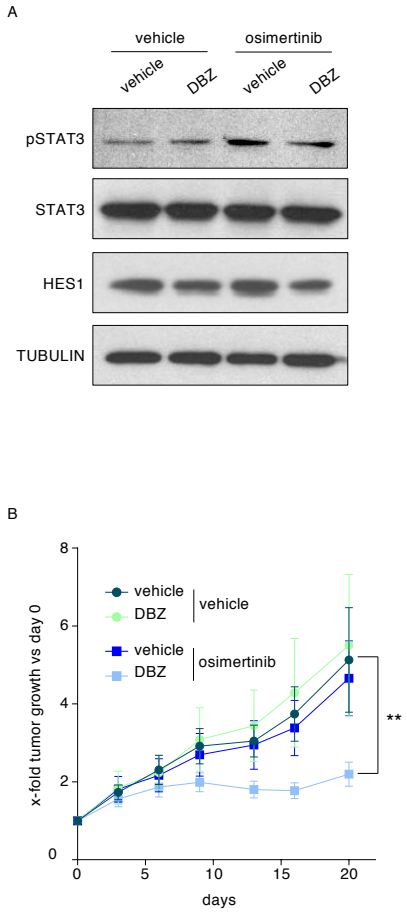

Figure. 6. Notch inhibition sensitizes *EGFR* ^{C797S} cells to osimertinib.

(A) Immunoblotting of the indicated proteins in PC9GROR cells treated with vehicle (DMSO) or DBZ (250 nM) and/or osimertinib (250 nM). **(B)** PC9GROR cells were

injected subcutaneously in the right flank of nude mice. The mice were then treated with vehicle (methocel, n = 8), DBZ (n = 8), osimertinib (n = 8), or the combination of DBZ and osimertinib (n = 7). The X-axis shows the tumor growth fold increase versus day 0. Values correspond to the average ± SEM. Statistical significance was determined by two-way ANOVA test followed by Tukey's post hoc test: * $p \leq 0.05$, ** $p \leq 0.01$. In the panel 6B, the comparison between DBZ and the combination or between osimertinib and the combination are also significant (respectively ** and *).

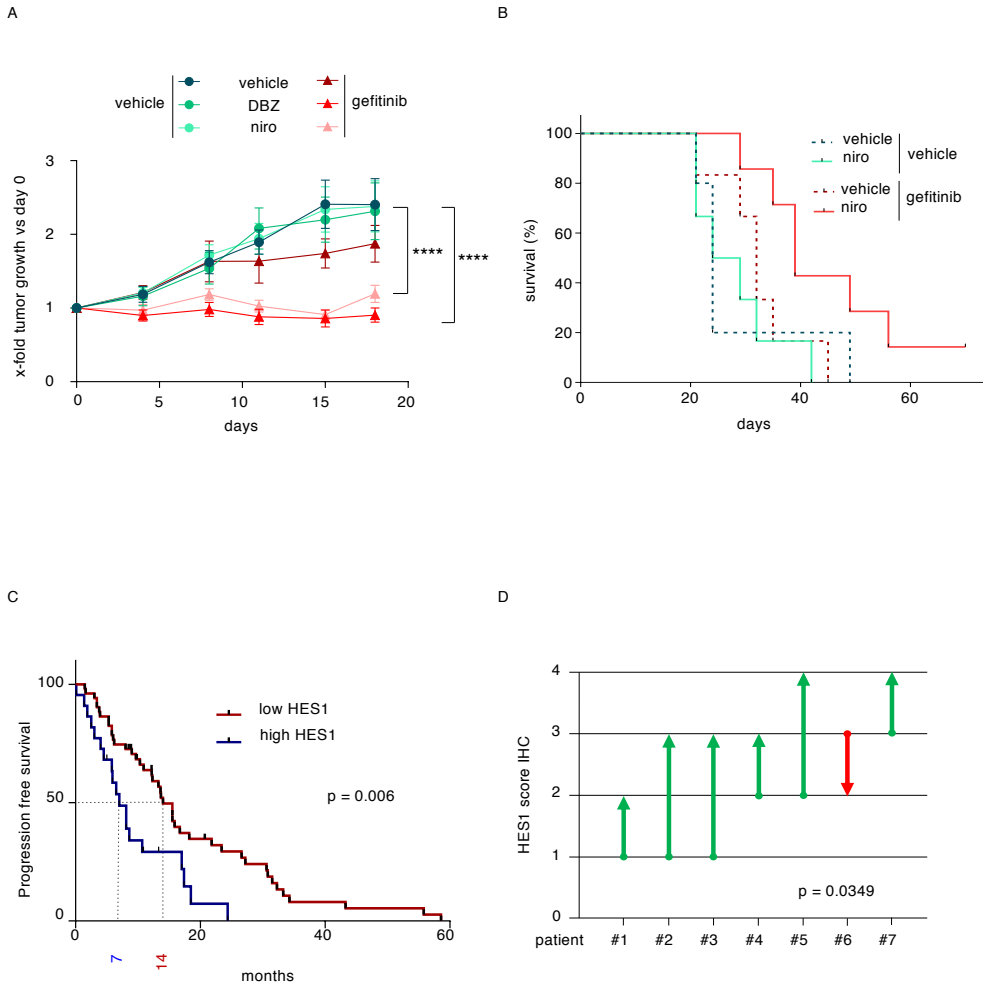

Figure. 7. High HES1 protein levels correlates with poor progression free survival and relapse in EGFR mutated lung adenocarcinoma patients under TKI treatment.

(A) PC9GR cells were injected subcutaneously on nude mice. The mice were then treated with vehicle (methocel, n = 6), DBZ (n = 6), nirogacestat (n = 6), gefitinib (n = 6) or the combination of DBZ and gefitinib (n = 7) or the combination of nirogacestat and gefitinib (n = 7). The X-axis shows the tumor growth fold increase versus day 0 and the Y-axis the days after treatment. Values correspond to the average ± SEM. Statistical significance was determined by a two-way ANOVA test followed by Tukey's post hoc test: * $p \leq 0.05$, ** $p \leq 0.01$, *** $p \leq 0.001$ and **** $p \leq 0.0001$. In the panel 7A, the comparison between DBZ and the combination DBZ/gefitinib or nirogacestat/gefitinib are also significant (respectively **** and ***) as well as nirogacestat compared with the combination DBZ/gefitinib or niro/gefitinib (respectively **** and ****). The comparison between gefitinib alone and the combination DBZ with gefitinib is also significant (**). **(B)** PC9GR cells were injected subcutaneously in nude mice. The mice were then treated with vehicle (methocel, n = 5), nirogacestat (n = 6), gefitinib (n = 6), or the combination of DBZ and gefitinib (n = 7). The X-axis shows the percentage of alive animals and the Y-axis the days after treatment. Statistical significance was determined by Gehan–Breslow–Wilcoxon test. Vehicle vs gefitinib (p = 0.3), vehicle vs nirogacestat (p = 0.93), vehicle vs the combination (p = 0.02), gefitinib vs the combination (p = 0.05) and nirogacestat vs the combination (p= 0.02). **(C)** Progression-free survival of EGFR TKI-treated patients with *EGFR*-mutated lung adenocarcinoma (n = 75) according to HES1 expression assessed by IHC staining (low HES1 = 0–2.50 HES1 score; high HES1 = 2.51–5.00 HES1 score). Statistical significance was determined by Gehan–Breslow–Wilcoxon test. **(D)** Representation of the change in HES1 immunohistochemical staining intensity score in patient samples before treatment (dot) and after relapse (arrowhead). Statistical significance was determined by paired two-tailed Student's t test.